

Chemical information from subsurface structures with 3-D Raman imaging and oil immersion objectives

Introduction

Confocal Raman imaging provides detailed information about samples with micron spatial resolution. The resulting images are based on molecular structure and are highly sensitive to small changes in chemical and physical properties. Additionally, confocal Raman imaging enables the non-destructive analysis of subsurface features in semi-transparent, non-turbid samples (up to several hundred micrometers deep depending on optical properties) without the need to cross-section or expose inner parts of the sample. By collating Raman images collected at different depths within a sample, it is possible to generate three-dimensional chemical images.

Collection of images from within a sample using standard (metallurgical) microscope objectives can introduce complicating factors not encountered during surface analysis, resulting in aberrations and reduced quality of results. When light passes through a material that has a refractive index greater than air ($n > 1$), paraxial light focuses differently from off-axis light (spherical aberration). This spherical aberration causes the focal point to be blurred (see Figure 1), and this effect escalates with increasing depth into the sample. Not only does this distort the actual sampling depth, causing the 3-D image to appear compressed along the z (focus) axis, but the spreading of the focus also causes a loss of spatial resolution and Raman intensity. The use of an aperture to achieve confocal imaging recoups some of this lost spatial resolution by limiting the collected signal to the region around the focal point, but with a reduction in Raman intensity. In short, traditional microscope objectives do not unlock the full 3-D imaging potential of Raman microscopy.

It is possible to correct this loss in fidelity using mathematical corrections; however, these vary in complexity and completeness in addressing the

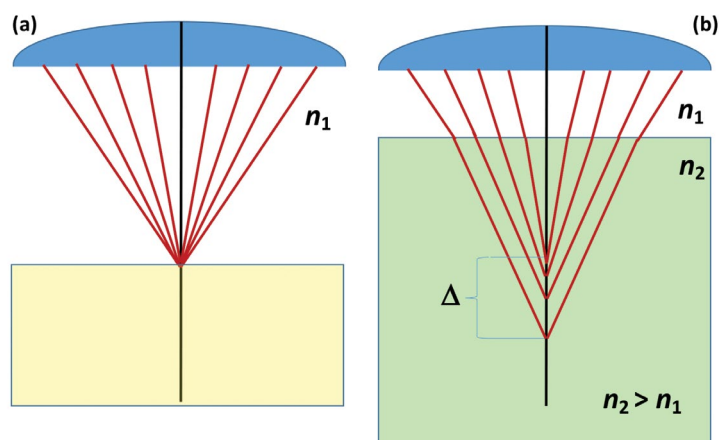


Figure 1. (a) Focus on a sample surface with air as the intermediate medium between the objective and the focal point. (b) Focus within a transparent sample with a higher index of refraction where spherical aberration causes a blurring of the focal point.

aberrations, and the loss of Raman intensity and spatial resolution are not recovered. Details of these mathematical and semi-empirical corrections can be found elsewhere and will not be discussed further in this paper.^{i,ii}

Alternately, the aberration can be addressed optically by using immersion objectives. By filling the gap between the objective and sample with an index matching fluid (rather than air), the spherical aberration can be reduced or eliminated. In essence, this removes the bending of the light at the surface of the sample and restores the lost spatial resolution and Raman intensity. Oil immersion objectives typically use oils that have an index of refraction around $n \approx 1.5$, a value similar to many polymeric materials. The use of oil also allows for a higher numerical aperture (better effective focus and resolution) and can increase the collected Raman intensity. Furthermore, oil immersion reduces the impact of sample shape and ultimately produces superior 3-D Raman imaging results.

This application note will present examples illustrating the use of an oil immersion objective with the Thermo Scientific™ DXR3xi Raman Imaging Microscope to improve the 3-D Raman imaging of buried or subsurface structures.

Experimental

3-D Raman images presented in this application note were created using a Thermo Scientific™ DXR3xi Raman Imaging Microscope and the accompanying Thermo Scientific™ OMNIC™xi Software. The OMNICxi Software contains both tools for straightforward collection of 3-D Raman data sets as well as built-in tools for the generation of the 3-D Raman images using interactive 3-D visualization features. The imaging data was collected using either an Olympus™ MPlanN 100X BD objective as the representative metallurgical objective or an Olympus™ PlanApo 100X oil immersion objective. The immersion oil used was non-fluorescent with an index of refraction of 1.516. A 532 nm laser with a power of 10 mW at the sample was used for all Raman images.

Results and discussion

A common application of Raman confocal depth analysis is the investigation of multi-layer polymer composites. The layered polymer composite selected for this example is approximately 124 μm thick and consists of 5 distinct layers. A 30 μm x 30 μm x 135 μm volume was analyzed with an image pixel size of 1 μm in x, y, and 1 μm steps in the z-direction using both the metallurgical and immersion

objectives. The immersion objective ultimately showed enhanced performance in three key aspects: accurate layer thickness measurement, increased signal-to-noise, and enhanced spectral purity.

Figure 2 shows the 3-D Raman images obtained using both a metallurgical objective (a) and an oil immersion objective (b). The figure shows Raman images based on MCR (multiplicative curve resolution). MCR analysis is a powerful approach because it allows OMNICxi to automatically segment layers without requiring any direct knowledge of the Raman spectral features of the components prior to analysis. As a reference, Figure 3 shows the results of 2-D imaging of a physical cross-section of the same polymer composite. When using the metallurgical objective, there is clearly a significant compression of the layers compared to what is observed in both the 3-D image using the oil immersion objective and the 2-D image obtained from the cross-section. The layer thicknesses determined from the 3-D image collected with the oil immersion objective and the 2-D image of the cross-section are in close agreement. It is also evident that the layers in the confocal 3-D image using the metallurgical objective are less well defined and suffer from a blurring of the focus and a loss of spatial resolution, leading to increased mixing of the spectral features at the interfaces. This also contributes to some additional uncertainty in terms of the thickness determinations. The use of an immersion objective produces superior results for measuring layer thickness.

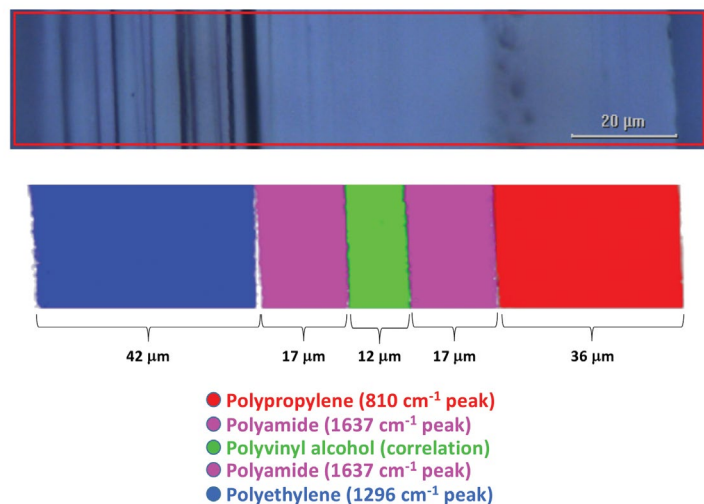
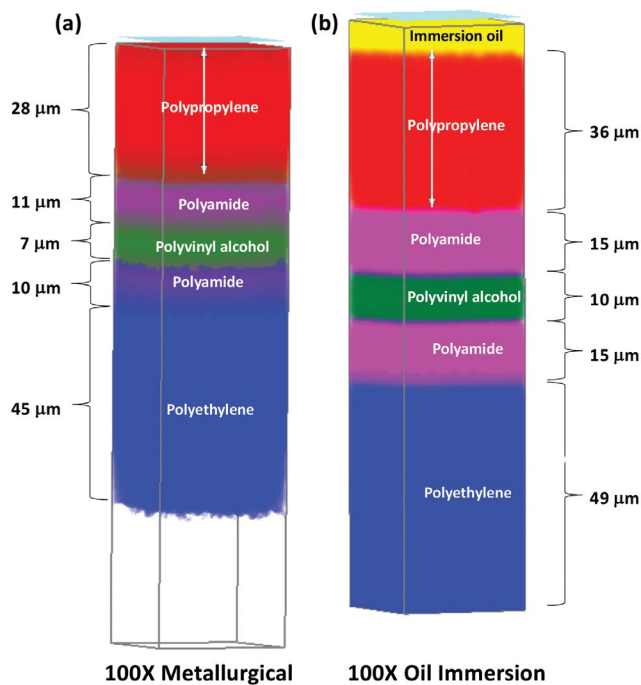


Figure 3. 2-D Raman image and visual image of a cross-section of the layered polymer composite. This reference measurement shows layer thicknesses that agree well with a 3-D Raman image using an oil immersion objective.

Figure 2. (a) 3-D Raman image based on a MCR analysis of a layered polymer composite film using a metallurgical objective. (b) 3-D Raman image based on a MCR analysis of the same layered polymer composite film using an oil immersion objective. The analysis with the oil objective shows clearer, more well-defined layers than with the metallurgical objective.

An additional advantage of using the oil immersion objective is a substantial increase in Raman intensity. Figure 4 shows a comparison of Raman spectra from a position in the middle of the polyvinyl alcohol layer from the two 3-D confocal imaging data sets. The oil immersion objective (green spectrum) provides spectra with approximately 3 times the Raman intensity and signal to noise ratio (S/N).

Finally, 3-D chemical images acquired with the immersion objective show better spectral separation between the various polymer layers. In this sample, the polyvinyl alcohol layer is sandwiched between two layers of polyamide, which have a strong Raman band at 1635 cm^{-1} . Comparing the relative intensity of this spectral feature to that of a polyvinyl alcohol band (1441 cm^{-1}) can be used as a measure of spectral separation. A reasonably pure polyvinyl alcohol spectrum acquired from the cross-section

image (Figure 5, blue trace) shows essentially no Raman feature at 1635 cm^{-1} . A spectrum of polyvinyl alcohol extracted from the 3-D volume using the metallurgical objective (Figure 5, red trace) shows a small but distinct contribution from polyamide, a result of spectral mixing between the layers; however, with the oil immersion objective (Figure 5, green trace) the relative contribution from the neighboring polyamide layers is significantly reduced. These results show that the oil immersion objective gives superior results for this type of 3-D confocal Raman depth imaging, resulting in more accurate layer thickness measurement, better spectral purity from each layer, and an overall increased signal-to-noise for the measurement. The results are comparable to the analysis of the cross-section without the need for the additional complexity of cross-sectioning the sample.

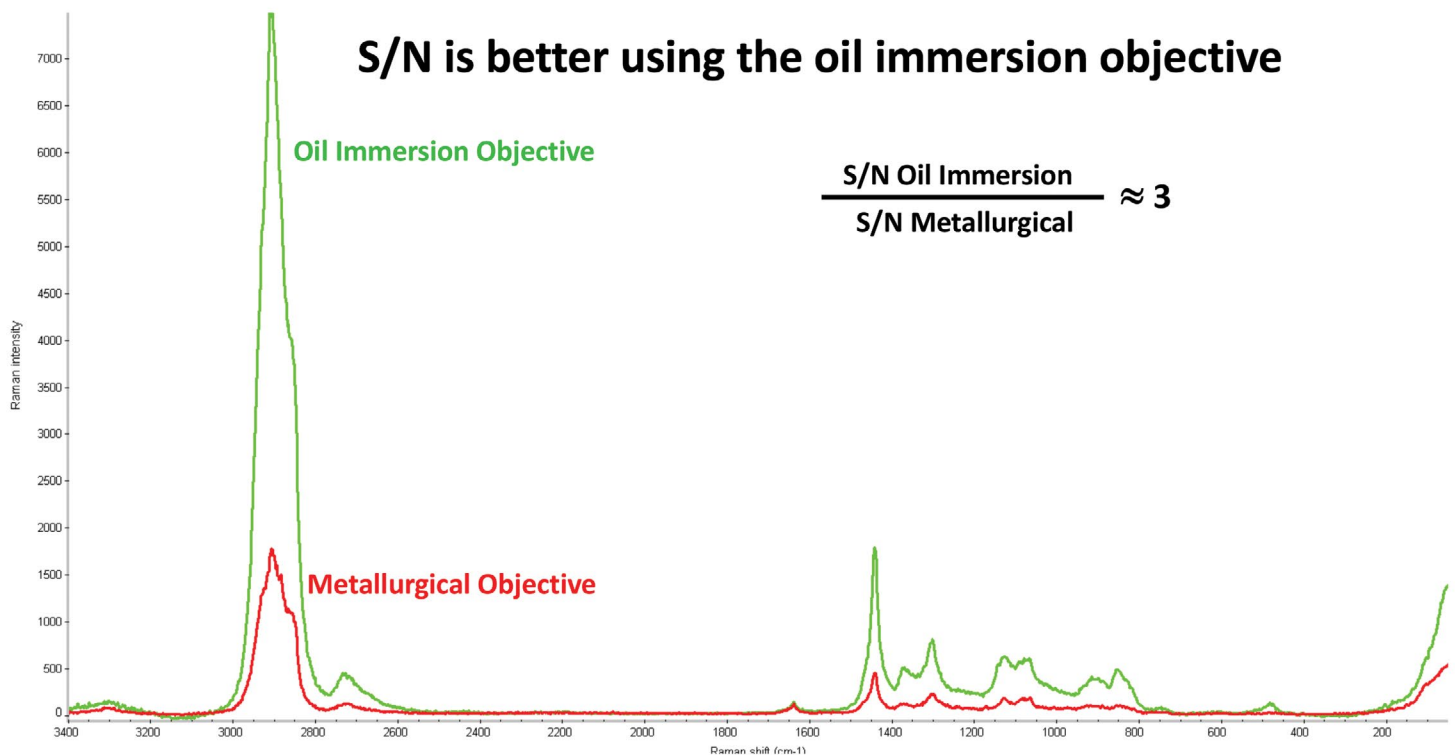


Figure 4. Spectra from the polyvinyl alcohol layer in the layered polymer composite film illustrating at least a 3-fold increase in both Raman intensity and signal to noise ratio (S/N). The S/N ratios were calculated from the intensity of the peak at 1441 cm^{-1} and the root mean squared noise calculated in the region from 2300-2200 cm^{-1} .

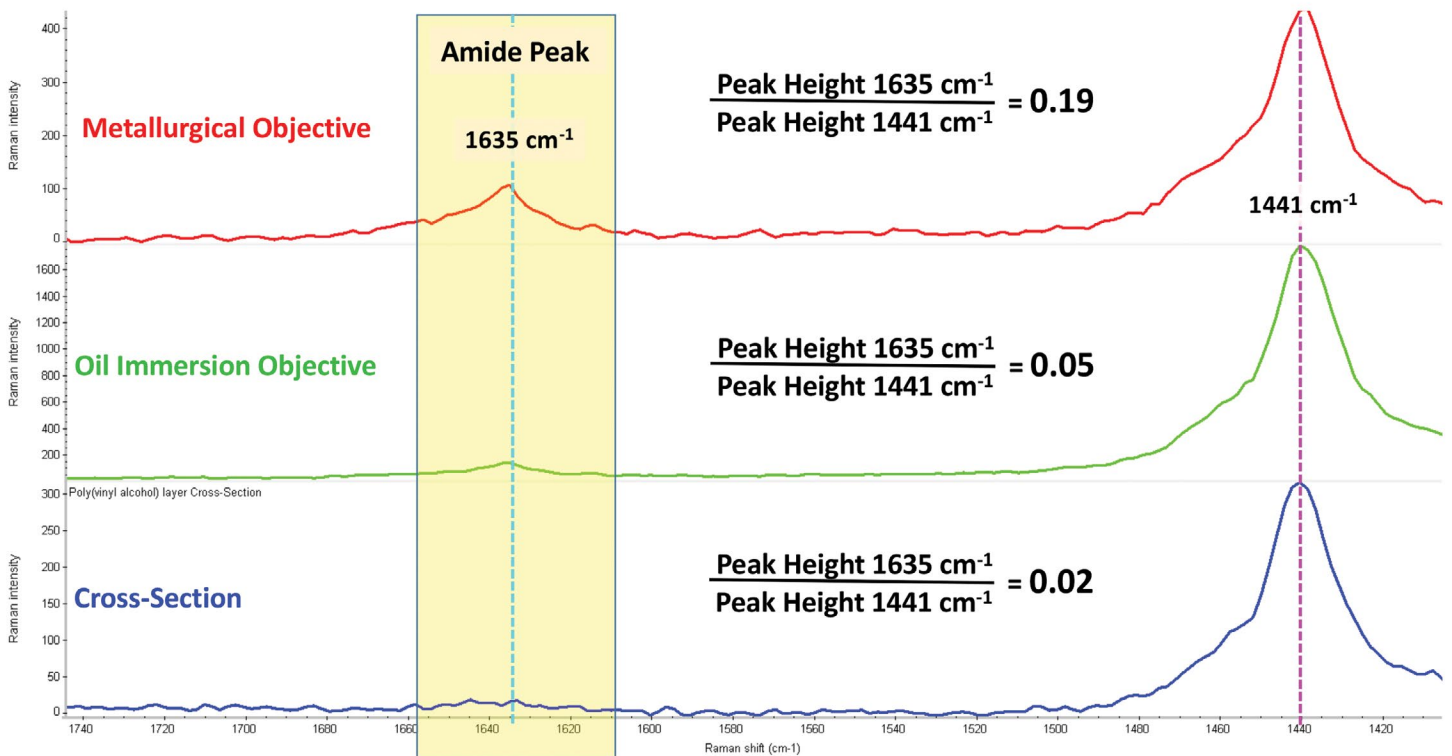


Figure 5. Spectra from the poly(vinyl alcohol) layer in the layered polymer composite film from the 3-D confocal data sets using both the metallurgical objective (red) and oil immersion objective (green) and from the 2-D image of the physical cross-section (blue). The peak height ratios ($1635\text{ cm}^{-1} / 1441\text{ cm}^{-1}$) give a measurement of the spectral contributions from the neighboring polyamide layers and illustrate the reduced spectral contributions of adjacent layers when using the oil immersion objective for 3-D confocal Raman imaging.

Non-planar shapes and surfaces can exacerbate the effects of refractive index differences, but immersion objectives can be applied to this situation as well. An example that illustrates this is the Raman imaging of polystyrene spheres that are approximately 25 microns in diameter (Polysciences, Inc.). A polystyrene sphere on a glass microscope slide was imaged using both a standard metallurgical objective and an oil immersion objective. The results are shown in Figure 6. With the metallurgical objective, there is an elongation and distortion long the z-axis (images c and d) for the bottom half of the sphere in addition to a significant loss of Raman intensity. This is a result of refraction and, to a lesser extent, reflection effects caused by the curved surfaces of the sphere and the refractive index difference as compared to the surrounding air. The same sphere imaged with an immersion objective (images a and b) shows a clear sphere without an elongated tail, as well as a more well-defined edge. This illustrates that the shape of the sample, combined with differences in refractive indexes, can introduce additional complicating factors when performing 3-D Raman imaging, but once again, the use of an oil immersion objective can help minimize these effects.

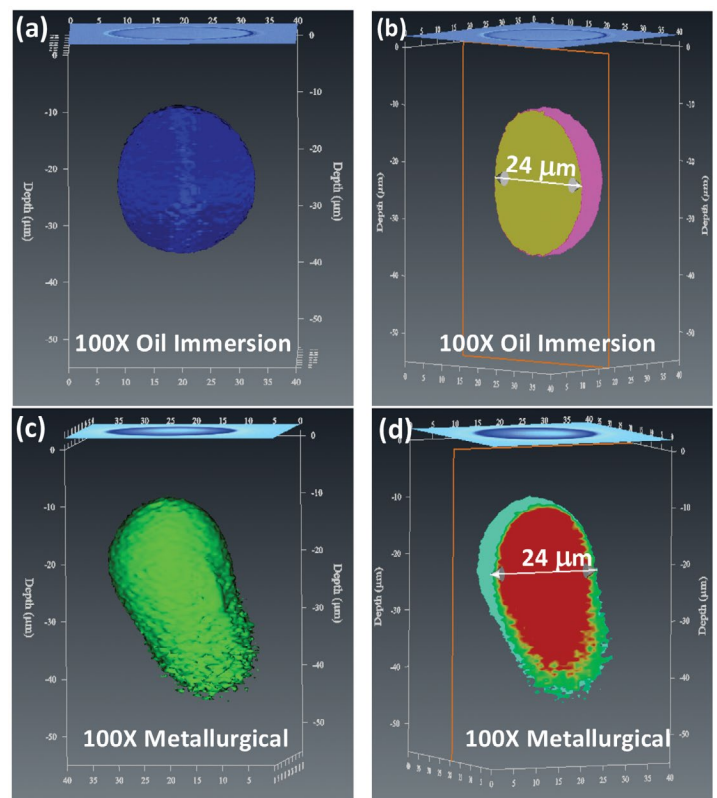


Figure 6. (a) & (b) Raman images of a $25\text{ }\mu\text{m}$ polystyrene sphere collected using an oil immersion objective, (c) & (d) Raman images of the same $25\text{ }\mu\text{m}$ polystyrene sphere collected using a metallurgical objective. The oil immersion images show an accurately reproduced sphere, while the metallurgical objective image shows significant distortion.

These principles extend to samples which have both distinct layers as well as non-planar features, such as a bi-component fiber. Bi-component fibers have two components that are not mixed together but have discrete arrangements (side by side, segmented, core-sheath, etc.) within the fiber and are engineered to take advantage of different properties of the constituents. The bi-component fiber imaged here has a core-sheath arrangement. The fiber is approximately 20 microns in diameter and has an outer sheath of Nylon 6 and an inner core of Nylon 6,6. Figure 7 shows the results of 3-D confocal imaging of the fiber using both a metallurgical objective (d,e,f) and an oil immersion objective (a,b,c). These images are also based on an MCR analysis. As with the polystyrene sphere example, the use of the metallurgical objective causes the Raman intensity to drop significantly toward the bottom

of the fiber, to the point that the bottom part of the fiber is not defined at all. There is also a clear uncertainty in the location of the boundary between the core and sheath. A 3-D image of the same fiber collected using an oil immersion objective reveals a well-defined, reasonably symmetric cross-section.

Attempts to physically cross-section this 20-micron fiber similarly to what was done with the layered polymer composite proved problematic. A straightforward method for mounting and cross-sectioning the fiber led to the physical deformation of the fiber. More rigorous mounting techniques, such as resin embedding, would have added significant time and complexity. 3-D confocal Raman imaging using the oil immersion objective provided a nondestructive solution that required no complex sample preparation.

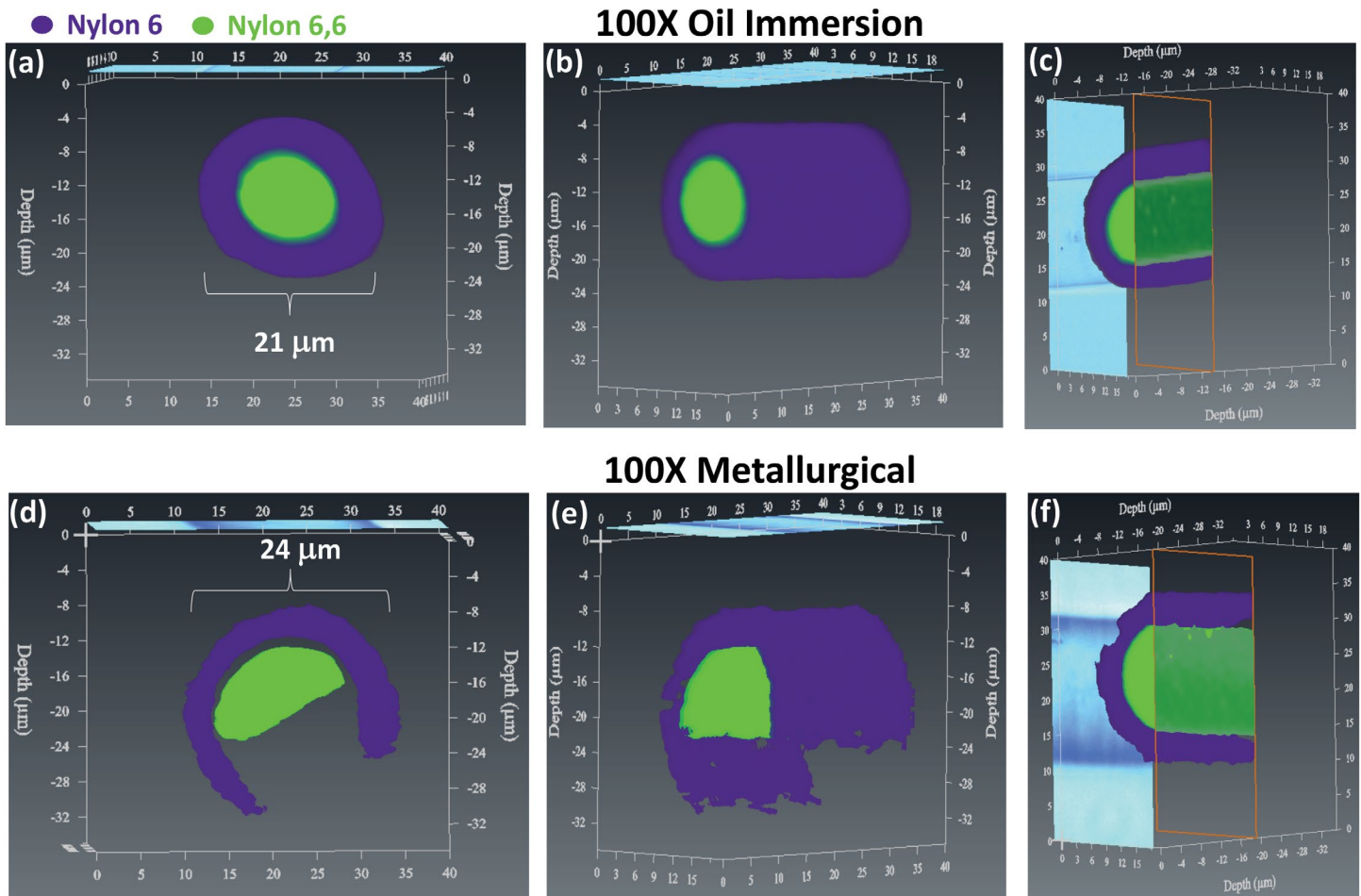


Figure 7. (a), (b), (c) Confocal 3-D Raman MCR images of a bi-component fiber (Nylon 6,6 (green) and Nylon 6 (purple), core-sheath arrangement) collected using an oil immersion objective. (d), (e), (f) Confocal 3-D Raman MCR images of the same bi-component fiber collected using a metallurgical objective. Views (c) and (f) show slices looking up along the z-axis of the 3-D Raman MCR images for the oil and metallurgical objectives respectively.

Conclusions

Confocal 3-D Raman imaging allows for subsurface imaging of semi-transparent samples without the need to physically expose the interior of the sample. While metallurgical objectives excel at surface analysis, they suffer from the effects of spherical aberration when used to probe the interior of samples. While the effects of spherical aberration can be partially accounted for by applying mathematical corrections, it is not possible to fully compensate for the loss of spatial resolution and Raman intensity. The use of oil immersion objectives is an effective strategy for optically addressing this problem and can increase subsurface imaging performance for many materials, including most polymers. Oil immersion objectives are standard accessories for DXR3 Raman microscopes, and their straightforward implementation can unlock the power of 3-D Raman imaging for your laboratory.

References

- i. N.Everall, *J. Raman Spectrosc.* **2014**, 45, 133-138
- ii. M.P. Miguel, J.P. Tomba, *J. Raman Spectrosc.* **2013**, 44, 447-452

Find out more at thermofisher.com/Raman

ThermoFisher
SCIENTIFIC